a dynamic model of oxytocin-receptor interaction and transduction.[4a,40,48] Studies are in progress to test these models by use of additional conformational restrictions[1,14] and by molecular dynamics simulations, coupled with NMR constraints.[49]

(48) (a) Meraldi, J.-P.; Hruby, V. J.; Brewster, A. I. R. *Proc. Natl. Acad. Sci. U.S.A.* **1977**, *74*, 1373. (b) Hruby, V. J.; Mosberg, H. I.; Hadley, M. E.; Chan, W. Y.; Powell, A. M. *Int. J. Peptide Protein Res.* **1980**, *16*, 372. (c) Hruby, V. J.; Mosberg, H. I. In *Neurohypophyseal Peptide Hormones and Other Biologically Active Peptides*; Schlesinger, D. H., Ed.; Elsevier/North Holland: New York, 1981; pp 211-226. (d) Hruby, V. J. In *Topics in Molecular Pharmacology*; Burgen, A. S. V., Roberts, G. C. K., Eds.; Elsevier/North Holland: Amsterdam, 1981; pp 99-126.

Acknowledgment. This work was supported by grants from the U.S. Public Health Service Grants to V.J.H. (NS-19972) and M.K. and from the National Science Foundation (V.J.H.). V.J.H. thanks the Guggenheim Foundation for a Fellowship that supported in part his research done at Harvard University. R.M.P. thanks the Robert A. Welch Foundation and the Texas Advanced Technology Research Projects Coordination Board for support.

Registry No. DPDPE, 88373-73-3.

(49) Brünger, P. T.; Clore, G. M.; Gronenborn, A. M.; Karplus, M. *Proc. Natl. Acad. Sci. U.S.A.* **1986**, *83*, 3801.

Side Chain Dynamics of Crystalline L-[3,3-$^2H_2$]Methionine Studied by Deuterium NMR Spectroscopy

S. W. Sparks, N. Budhu,† P. E. Young,† and D. A. Torchia*

Contribution from the Bone Research Branch, National Institute of Dental Research, National Institutes of Health, Bethesda, Maryland 20892, and the Department of Chemistry, York College, City University of New York, Jamaica, New York 11451. *Received April 21, 1987*

Abstract: In order to better understand the dynamics of the side chain of methionine, we have measured and analyzed ^2H nuclear magnetic resonance line shapes and spin-lattice relaxation times in polycrystalline L-[3,3-$^2H_2$]methionine from -35 to +106 °C. At -35 °C, the C^β-^2H bond axes are nearly rigid and execute only small amplitude librations. However, at temperatures above 0 °C, two dynamically distinct types of methionine side chains, designated A and B, are observed and are assigned to the two crystallographically different methionine side chains found in the unit cell. The values of the generalized order parameters of the A and B side chains decrease from unity at -35 °C to 0.69 and 0.25, respectively, at 106 °C. At 38.45 MHz, we are able to analyze all the data obtained for both types of side chains using a two-site jump model. Using this model we find the respective A side chain and B side chain correlation times decrease from 0.45 to 0.019 ns and from 4.2 to 0.049 ns in the -19 to 77 °C temperature range. The apparent activation energy for the A side chain is 21.6 ± 8.3 kJ/mol, whereas the apparent activation energy of the B side chain is 30.9 ± 1.6 kJ/mol below 31 °C and 30.9 ± 4.9 kJ/mol above 50 °C. The Arrhenius plot of the B side chain correlation times is nonlinear in the 30-50 °C range, where crystalline methionine undergoes a phase transition. At temperatures above 50 °C, the analysis of the ^2H line shapes shows that the populations of the two sites are nearly equal and that the jump angle is ca. 90°. Using a modified two-site jump equation and a six-site computer calculation to analyze the field (at 38.45 and 76.77 MHz) and orientation dependence of T_1 at low temperature, we find that the jump angle remains fixed at ca. 90° but that the difference in relative populations of the two sites approaches unity as the temperature decreases from 24 to -35 °C. Because the 90° jump angle corresponds approximately to jumps on a tetrahedral lattice, we conclude (a) that the C^α-C^β bond of the B side chain undergoes rapid trans-gauche isomerization and (b) that the trans isomer is the predominate species below 0 °C, while the isomer populations are nearly equal above 50 °C.

The recent interest in understanding the internal dynamics of proteins[1,2] has stimulated studies of amino acid side chain dynamics in crystalline amino acids[3-8] and peptides.[9,10] At first sight, the stable crystals formed by these compounds would appear to offer unfavorable habitats for molecular motion. However, significant motions have been observed for a number of side chains of hydrophobic amino acids (e.g., Phe, Tyr, Pro, and Met) in the crystalline state. Motions of side chains of hydrophobic residues are of particular interest, because these residues are often buried within proteins. Therefore, studies of motions of hydrophobic side chains of amino acids in the crystalline state can provide information about possible internal motions within proteins.

Among the side chain motions studied so far, the motions of the side chain of L-methionine are the most complex and potentially interesting. Large changes in the line shapes of the methyl deuterons are observed in ^2H NMR spectra of crystalline L-[*methyl*-$^2H_3$]methionine in the 10-80 °C temperature range.[4] It has been shown[4,11] that these changes in line shape are not due to either rotation about the S-C^ϵ bond (the changes in line shape caused by methyl rotation occur at temperatures below -130 °C) or motions involving reorientation of the C^α-H bond. Therefore motions about the C^α-C^β, C^β-C^γ, and/or C^γ-S bonds are responsible for the observed changes in methyl deuteron line shapes.

* National Institutes of Health.
† York College.

(1) Gurd, F. R. N.; Rothgeb, T. M. *Adv. Protein Chem.* **1979**, *33*, 73-165.
(2) Karplus, M.; McCammon, J. A. *CRC Crit. Rev. Biochem.* **1981**, *9*, 293-349.
(3) Gall, C. M.; DiVerdi, J. A.; Opella, S. J. *J. Am. Chem. Soc.* **1981**, *103*, 5039-5043.
(4) Keniry, M. A.; Rothgeb, T. M.; Smith, R. L.; Gutowsky, H. S.; Oldfield, E. *Biochemistry* **1983**, *22*, 1917-1926.
(5) Torchia, D. A. *Annu. Rev. Biophys. Bioeng.* **1984**, *13*, 125-144.
(6) Shaefer, J.; Stejskal, E. O.; Mackay, R. A.; Dixon, W. T. *J. Magn. Reson.* **1984**, *57*, 85.
(7) Hiyama, Y.; Silverton, J. V.; Torchia, D. A.; Gerig, J. T.; Hammond, S. J. *J. Am. Chem. Soc.* **1986**, *108*, 2715-2723.
(8) Sarkar, S. K.; Young, P. E.; Torchia, D. A. *J. Am. Chem. Soc.* **1986**, *108*, 6459-6464.
(9) Rice, D. M.; Wittebort, R. J.; Griffin, R. G.; Meriovitch, E.; Meinwald, Y.; Freed, J. H.; Scherage, H. A. *J. Am. Chem. Soc.* **1981**, *103*, 7707-7710.
(10) Sarkar, S. K.; Torchia, D. A.; Kopple, K. D.; VanderHart, D. L. *J. Am. Chem. Soc.* **1984**, *106*, 3328-3331.
(11) Batchelder, L. S.; Niu, C. H.; Torchia, D. A. *J. Am. Chem. Soc.* **1983**, *105*, 2228-2231.

0002-7863/88/1510-3359$01.50/0

Motions of the methionine side chain are probably closely related to reported structural changes in the L-methionine crystals. L-Methionine crystals undergo a solid-state phase transition at ca. 32–33 °C,[12] and the volume of the crystal lattice gradually increases as the temperature increases from −20 to 95 °C.[13]

In order to better understand the complex dynamics of the methionine side chain, we have used solid-state ^2H NMR spectroscopy to study the crystalline amino acid specifically enriched with ^2H at the β carbon. We report herein β-deuteron NMR equilibrium line shapes and inversion–recovery line shapes obtained from −35 to 106 °C. Using a two-site jump model to analyze the data, we derive order parameters and correlation times for motions of the C^β–^2H bond axes of the two inequivalent molecules in the unit cell.

Although the two-site jump model accounts for all of the line shape data and for the relaxation measurements when $(\omega\tau)^2 \ll 1$ (ω is the Larmor precession frequency and τ is the correlation time) the model fails to provide a self-consistent analysis of the relaxation data when $\omega\tau \simeq 1$. We show that this occurs because this simple model slightly overestimates $1/T_1$. We further show that this deficiency in the model can be remedied by a simple modification of the two-site jump equation for $1/T_1$. Using this modified equation, we can account for the observed field dependence and angular dependence (T_1 anisotropy) of T_1. This enables us to determine the relative populations of the two sites as well as the angle, $2\theta_0$, made by the C^β–^2H bond axes in the two sites.

Experimental Section

DL-[3,3-$^2H_2$]Methionine was prepared from commercial methionine by the method of Billington et al.[14] The racemic mixture was enzymatically resolved according to the procedure in Greenstein and Winitz[15] as follows:

Acetyl-DL-[3,3-$^2H_2$]methionine. The synthetic DL-[3,3-$^2H_2$]methionine (2.0 g, 0.013 mol) was dissolved in glacial acetic acid (27 mL) with heating. The solution was cooled and acetic anhydride (2.0 g, 0.02 mol) was added in portions. The mixture was boiled for several minutes and the solvent removed in vacuo at 40 °C. The syrupy residue was washed three times with small portions of water and benzene and then dissolved in anhydrous ether (10 mL) and stored overnight at 0 °C. Crystals of acetyl-DL-[3,3-$^2H_2$]methionine were collected (2.50 g, 0.013 mol, 98%).

L-[3,3-$^2H_2$]Methionine. Acetyl-DL-[3,3-$^2H_2$]methionine (2.49 g, 0.013 mol) was dissolved in doubly distilled water (138 mL) and the pH adjusted to 7.16 with 25% NH_4OH. Porcine kidney acylase I (3.0 mg, grade II, Sigma Chemical Co.) powder was added and the digest placed in a 37 °C water bath for 24 h. The mixture was then shaken with glacial acetic acid (1.35 mL) and was filtered by vacuum with the aid of decolorizing carbon. The resulting solution was evaporated to 10 mL in vacuo and absolute ethanol (36 mL) was added. The resulting white crystals (0.32 g, 0.0021 mol, 33%) were collected $[\alpha]^{22}$ +23.6 (c = 6.33 g/100 mL, 6 N HCl). Labeling selectivity was determined by ^1H NMR to be greater than 99.5%.

Optical purity was determined by HPLC of the derivitized amino acid. With use of the procedure of Marfey,[16] 5 μmol of sample were reacted with 1-fluoro-2,4-dinitrophenyl-5-L-alanine amide (FDAA). The resulting product was dried, dissolved in DMSO, and separated by reverse-phase HPLC. Elution was accomplished in 30 min with a 10–50% gradient of aqueous 50 mM triethylamine phosphate, pH 3.0, in acetonitrile with use of a Waters C_{18} column. Optical purity, determined from integrated peak area and peak heights at 340, 280, and 254 nm, is better than 98%.

Before use, the amino acid was recrystallized from distilled water. Crystals were selected from the mother liquor, air dried, and ground to a powder. Approximately 40 mg of powder was packed into a 5-mm glass NMR tube and used for all further NMR measurements.

Solid-state ^2H NMR spectra were obtained at 6 T (38.45 MHz) on a home-built spectrometer described previously.[17] Spectra at 12 T (76.77 MHz) were obtained on a NIC-500 spectrometer modified for solid-state work.[7] Deuterium line shapes were acquired with the quadrupole echo pulse sequence[18] and spin–lattice relaxation times determined by the inversion–recovery method with a quadrupole echo detection sequence.

Nominal acquisition conditions and parameters were as follows: temperature range, −35 to +106 °C; number of acquisitions, 512–4096; $\pi/2$ pulse, 2.0–2.5 μs; acquisition recycle time, 60 ms to 3 s. All free induction decays were acquired with 2048 points per channel at a 2-MHz sampling rate and transformed with 1–2 kHz of line broadening.

Simulations of deuterium powder line shapes were calculated on a VAX 750 computer. The principal frequencies of the experimental spectra were measured directly and fast limit powder line shapes calculated with the standard formulas.[19] Inversion–recovery spectra were simulated by calculating the partially relaxed signal intensity for each orientation of B_0. The reorientation correlation time was varied until agreement was found with experimental spectra. All calculated line shapes included corrections for finite pulse power using the formulas from Hiyama et al.[7] and Bloom et al.[20]

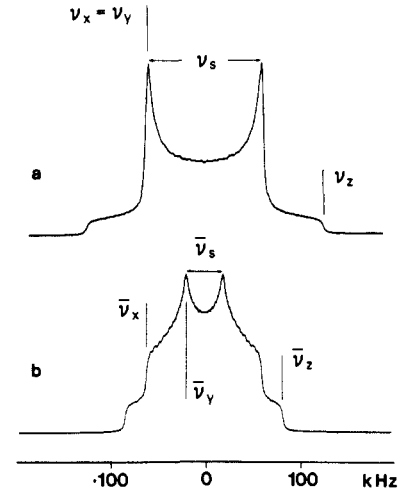

Figure 1. Calculated ^2H NMR line shapes for polycrystalline materials: (a) axially symmetric, $\eta = 0$, Pake pattern corresponding to immobile C–^2H bonds with principal frequencies $\nu_x = \nu_y = -60$ kHz, $\nu_z = 120$ kHz; (b) axially asymmetric pattern resulting from fast exchange of C–^2H bonds between two orientations. Motionally averaged principal frequencies are $\bar{\nu}_x = -60$, $\bar{\nu}_y = -20$, and $\bar{\nu}_z = 80$ kHz with quadrupolar splitting $\bar{\nu}_s = 40$ kHz. The two bond orientations, equally populated, are separated by jump angle $2\Theta_0 = 56.25°$. Both calculations assume an axially symmetric electric field gradient tensor with unique axis parallel to the C–^2H internuclear vector and a quadrupole coupling constant, $e^2qQ/h = 4\nu_q/3$, of 160 kHz.

Theory

The deuteron is a spin $I = 1$ nucleus possessing a magnetic dipole and electric quadrupole. In the absence of an electric field gradient, the interaction of the nuclear dipole moment with an external magnetic field, B_0, determines the resonance frequency of the two degenerate transitions.

When deuterium is chemically bound to another atom, such as carbon, the electric field gradient (EFG) of the bond interacts with the electric quadrupole of the deuteron to produce a shift in resonance frequency. The shift in frequency, which depends on the relative orientation of B_0 and the EFG tensor, is expressed as

$$\nu = \nu_q(3\cos^2\theta_0 - 1 - \eta\sin^2\theta_0\cos 2\phi_0)/2 \qquad (1)$$

where $4\nu_q/3$ is the quadrupole coupling constant, e^2qQ/h, η is the asymmetry parameter of the EFG tensor, and θ_0 and ϕ_0 are the spherical polar angles defining the orientation of B_0 in the EFG tensor principal axis system. When the bond is predominantly σ in character, as with carbon, the asymmetry parameter is small, $\eta < 0.05$, with the unique tensor axis lying parallel to the inter-

(12) Hutchens, J. O.; Cole, A. G.; Stout, J. W. *J. Biol. Chem.* **1964**, *239*, 591–595.
(13) Curto, E. V.; Dahlquist, F. W. *Biophys. J.* **1987**, *51*, 461a.
(14) Billington, D. C.; Golding, B. T.; Kebbell, M. J.; Nassereddin, I. K. *J. Lab. Comp. Radiopharm.* **1981**, *18*, 1773–1784.
(15) Greenstein, J. P.; Winitz, M. *Chem. amino Acids* **1961**, *3*.
(16) Marfey, P. *Carlsberg Res. Commun.* **1984**, *49*, 591–596.
(17) Sarkar, S. K.; Sullivan, C. E.; Torchia, D. A. *J. Biol. Chem.* **1983**, *258*, 9762–9767.
(18) Davis, J. H.; Jeffery, K. R.; Bloom, M.; Valic, M. I.; Higgs, T. P. *Chem. Phys. Lett.* **1976**, *42*, 390–394.
(19) Spiess, H. W. *NMR Basic Principles and Progress*; Springer-Verlag: Berlin, 1978; Vol. 15.
(20) Bloom, M.; Davis, J. H.; Valic, M. I. *Can. J. Phys.* **1980**, *58*, 1510–1517.

nuclear vector, and with very good approximation

$$\nu = \nu_q(3\cos^2\theta_0 - 1)/2 \quad (2)$$

For the polycrystalline samples used in this study, all crystallite orientations occur with equal probability and each C–^{2}H bond orientation is equally represented. The ^{2}H NMR spectrum, a superposition of signals from each crystallite, is a Pake pattern (Figure 1a).[21] The spectrum is symmetric with respect to the center frequency because the quadrupole interaction raises the frequency of one transition while lowering the frequency of the other. Spectrum discontinuities appear when the B_0 field direction lies parallel to one of the EFG tensor axes. The coupling constant, e^2qQ/h, is typically 170 kHz for C–^{2}H bonds, resulting in discontinuities at $\nu_x = \nu_Y = 64$ kHz and $\nu_z = 128$ kHz. For this case of $\eta = 0$ and a fixed orientation for each C–^{2}H bond in the polycrystalline sample, the separation of spectrum maxima, ν_s, equals ν_q.

If the C–^{2}H bonds reorient, the quadrupole interaction is modulated, causing both spin–lattice relaxation and modification of the static deuterium line shape.[19,21] The shape of the motionally averaged deuterium powder pattern is easily calculated if the exchange rate between bond orientations is much greater than the quadrupole coupling constant. In this fast motion limit, the observed deuterium frequency is the average of the deuterium frequency in each orientation weighted by the relative equilibrium population of that orientation. The averaged frequency can be written

$$\bar{\nu} = \bar{\nu}_q(3\cos^2\theta - 1 - \bar{\eta}\sin^2\theta\cos 2\phi)/2 \quad (3)$$

where θ and ϕ define the orientation of B_0 in the motionally averaged EFG tensor principal axis system, and where $\bar{\nu}_q$ and $\bar{\eta}$ are the motionally averaged values of ν_q and η.

As a consequence of eq 3, the fast limit line shape is specified by the three motionally averaged principal frequencies $\bar{\nu}_x$, $\bar{\nu}_y$, $\bar{\nu}_z$. In the motionally averaged ^{2}H powder pattern, a discontinuity is observed at each principal frequency, corresponding to B_0 oriented along one of the principal axes of the averaged EFG tensor. Because the trace of the motionally averaged EFG tensor is zero,

$$\bar{\nu}_x + \bar{\nu}_y + \bar{\nu}_z = 0 \quad (4)$$

In addition, the squares of the averaged principal frequencies are related to S^2, the square of the generalized order parameter,[22,23] according to

$$2(\bar{\nu}_x^2 + \bar{\nu}_y^2 + \bar{\nu}_z^2)/(3\nu_q^2) = S^2 \quad (5)$$

When rapid exchange takes place between two bond orientations, $\hat{\mu}_1$ and $\hat{\mu}_2$ depicted in Figure 2, the following condition also applies

$$|\bar{\nu}_i| = \nu_q/2 \quad (6)$$

where $i = x$ if $|\bar{\nu}_z| \geq \nu_q/2$, otherwise $i = z$.

Equations 4–6 show that the information content of a fast-limit two-site powder pattern is S^2. The order parameter is related to the equilibrium relative populations of the two sites, P_1 and P_2, and to the angle between the two bond orientations, $2\theta_0$, according to eq 7. Equation 7 shows that a line shape analysis provides

$$S^2 = 1 - 3P_1P_2\sin^2(2\theta_0) \quad (7)$$

information about the amplitude of molecular motion. This information is supplemented by ^{2}H spin–lattice relaxation measurements. The ^{2}H relaxation time in the case of two-site exchange is given by[24]

$$1/T_1 = (\bar{\omega}_q^2/6)(1 - S^2)\{g(\tau,\omega) \times [B_4 - (0.75B_1 - B_2)\cos 2\phi] + g(\tau,2\omega)[4B_5 - 4B_2\cos 2\phi]\} \quad (8)$$

where $\bar{\omega}_q = 2\pi\bar{\nu}_q$, the correlation time, τ, is defined as the inverse

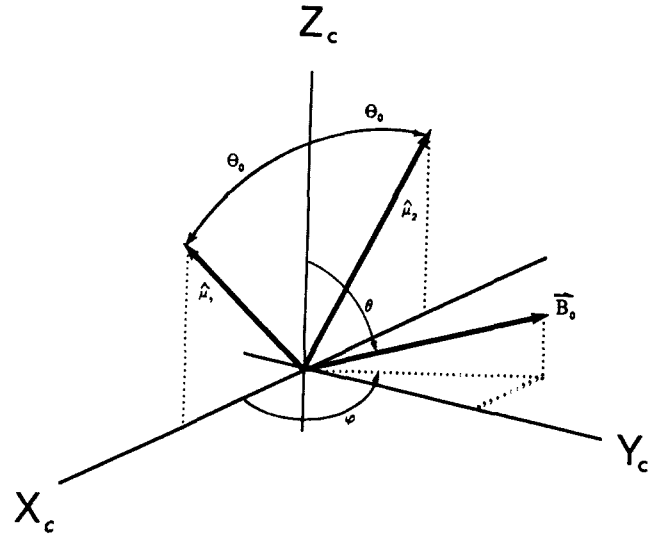

Figure 2. The unit vector $\hat{\mu}$ lies along the C–^{2}H bond. Exchange of $\hat{\mu}$ between orientations $\hat{\mu}_1$ and $\hat{\mu}_2$ averages the principal values of the ^{2}H EFG tensor. The two orientations shown here are defined by polar angles $\Theta = \Theta_0$ and $\Phi = 0°$, 180° in the crystal fixed axis system (X_c,Y_c,Z_c). The orientation of the applied static field, B_0, is defined by polar angles θ and ϕ.

of the sum of jump rates, $[k_{12} + k_{21}]^{-1}$, $g(\tau,\omega) = \tau/(1 + (\omega\tau)^2)$, ω is the Larmor frequency, and B_i are angular coefficients defined in ref 24. In the extreme narrowing limit, $(\omega\tau)^2 \ll 1$, eq 8 simplifies to

$$1/T_1 = (\bar{\omega}_q^2\tau/3)(1 - S^2)(1 + 3\sin^2\theta\sin^2\phi) \quad (9)$$

where θ and ϕ are the polar angles of B_0 in the crystal fixed coordinate system (X_c,Y_c,Z_c) depicted in Figure 2. For C–^{2}H bonds, the large quadrupole coupling constant makes quadrupole relaxation the dominant T_1 mechanism, allowing the neglect of other relaxation mechanisms.[19]

Because S^2 is given by the averaged principal frequencies, it is clear from eq 8 and 9 that a T_1 measurement yields the correlation time. In addition, when $(\omega\tau)^2 \geq 1$, measurement of the angular dependence of T_1 (the T_1 anisotropy) provides information about the orientation of the motionally averaged EFG principal axes that are orthogonal to Y_c. This information, together with eq 5 and 7, permits one to determine Θ_0 and the relative populations of the two sites. This statement does not apply when $(\omega\tau)^2 \ll 1$ because, according to eq 8, T_1 is invarient to rotation of B_0 about Y_c in this case.

The above equations summarize essential features of the two-site jump model. They establish relations between experimental line shapes and relaxation times, and the parameters that define the model: site populations, P_1 and P_2; jump angle, $2\Theta_0$; and correlation time, τ. These parameters are used in this study to characterize the C$^\beta$–^{2}H bond reorientation in L-[3,3-^{2}H$_2$]-methionine.

A motional model is also considered in which C$^\beta$–^{2}H bonds librate in a cone having semiangle Θ_c. The deuterium line shape remains axially symmetric and the motionally averaged quadrupole splitting, $\bar{\nu}_q$, is related to the static splitting, ν_q, by

$$\bar{\nu}_q = \nu_q\cos\Theta_c(1 + \cos\Theta_c)/2 \quad (10)$$

Results and Discussion

Deuterium NMR line shapes of polycrystalline L-[3,3-^{2}H$_2$]-methionine obtained over the temperature range −35 to +106 °C are shown in Figure 3. The −35 °C spectrum is an axially symmetric powder pattern having a 120-kHz quadrupole splitting, a value close to that typical of a static C–^{2}H bond. This observation indicates that large-amplitude reorientation of the C$^\beta$–^{2}H bond does not occur at this temperature. Spectra at higher temperatures are seen to be the superposition of two powder patterns, A and B, with approximately equal areas but significantly different line shapes and quadrupolar splittings (Figure 4). The retention

(21) Abragam, A. *The Principles of Nuclear Magnetism*; Oxford: London, 1961.
(22) Lipari, G.; Szabo, A. *J. Am. Chem. Soc.* **1982**, *104*, 4546–4559.
(23) Torchia, D. A.; Szabo, A. *J. Magn. Reson.* **1985**, *64*, 135–141.
(24) Torchia, D. A.; Szabo, A. *J. Magn. Reson.* **1982**, *49*, 107–121.

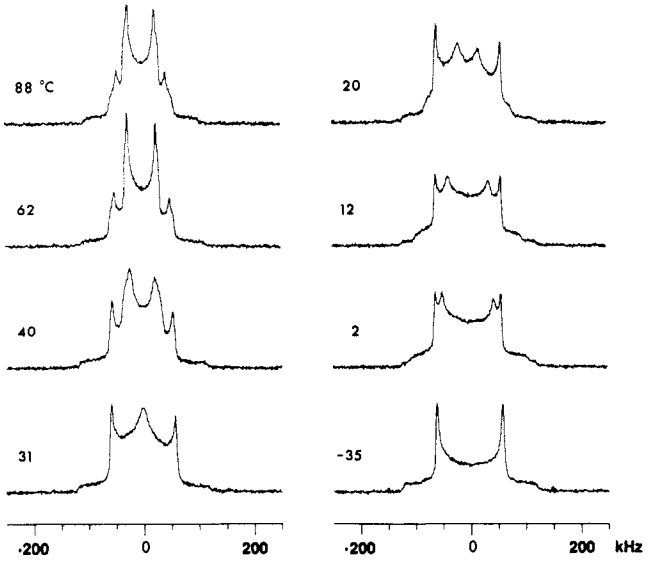

Figure 3. The temperature dependence of the ^2H line shape in polycrystalline L-[3,3-$^2H_2$]methionine. Spectra were acquired with an approximately 40-mg sample, 1024 acquisitions, and 1-s recycle time at 38.45 MHz.

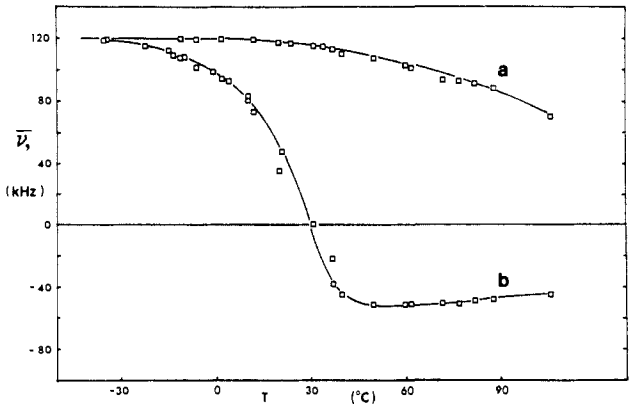

Figure 4. Motionally averaged quadrupolar splittings, $\bar{\nu}_s$, are plotted against temperature for A molecule (a) and B molecule (b) powder patterns. In order to achieve a smooth temperature dependence of $\bar{\nu}_q$, the quadrupolar splitting for the B molecule powder pattern was assumed to be negative above 30 °C.

of near axial symmetry, $\bar{\nu}_s \geq 100$ kHz, in one pattern over most of the temperature range indicates that for one-half of the C^β–^2H bonds, reorientation is highly restricted. In contrast, the great reduction in $\bar{\nu}_s$ in the second pattern, Figure 4, is evidence of considerable motional freedom for the other C^β–^2H bonds.

The observation of two populations of L-methionine side chains having different motional behavior is similar to observations made on L-phenylalanine.[3,5,6] However, unlike L-phenylalanine which crystallizes in two forms, each having its own motional characteristics, L-methionine crystallizes in a single form containing two crystallographically distinct molecules.[25] The two NMR powder patterns, then, are due to methionine side chains occurring in different molecular environments within a single-crystal lattice.

An X-ray structure study[25] has shown that the methionine molecules in the crystal lattice are arranged in double layers with backbone atoms hydrogen bonded in a polar layer and the side chains facing each other in a hydrophobic layer. The unit cell contains four molecules: two A molecules, each with its side chain in a trans-trans-trans conformation, and two B molecules with each side chain having a trans-gauche-gauche conformation. The temperature factors of the side chain atoms of the B molecules are much greater than those for A molecules, indicating that the B side chain is the more disordered. We therefore assign the most

Table I. Motionally Averaged Principal Frequencies (kHz) in L-[3,3-$^2H_2$]Methionine[a]

	A side chain			B side chain		
temp (°C)	$\bar{\nu}_x$	$\bar{\nu}_y$	$\bar{\nu}_z$	$\bar{\nu}_x$[b,c]	$\bar{\nu}_y$	$\bar{\nu}_z$[c]
−19	−60.0	−59.5	119.5			
−15				−60.6	−55.7	116.2
−10				−61.2	−53.9	115.1
−1	−60.0	−59.0	119.0			
+1	−60.8	−59.9	120.7			
4				−60.5	−46.4	107.2
10				−60.9	−41.3	102.2
20	−60.0	−58.7	118.7			
21	−60.0	−58.8	118.8	−60.9	−23.8	84.6
31				−62.0	0.0	62.0
36	−61.4	−56.0	117.4	−58.6	19.4	38.9
50	−60.0	−52.0	112.0	−57.9	25.9	32.0
60	−61.0	−50.8	111.8	−57.9	26.0	31.9
62	−59	−50	110	(−59)	26	33
72	−60	−49	109	(−57)	25	32
77	−60.0	−47.0	107.0	−57.1	25.4	31.7
82	−60	−47	107	(−57)	25	32
88	−59	−44	103	(−56)	24	32
106	−59	−38	97	(−56)	23	33

[a] Typical uncertainties in measured prinmcipal frequencies are 1–2 kHz. [b] The values in parentheses were calculated from experimental data using eq 4. [c] In order to follow the convention[19] that $|\nu_z| \geq |\nu_x| \geq |\nu_y|$, the x and z subscripts must be interchanged at temperatures above 31 °C.

temperature sensitive powder pattern, the B pattern, to the β deuterons on the B molecule.

In contrast to the side chain atoms, the backbone atoms have small temperature factors, suggesting an ordered methionine backbone. In agreement with this result, ^2H NMR studies[4] have shown that up to at least 45 °C, the powder line shape of the α-deuteron in L-[2-^2H]methionine is a rigid lattice Pake pattern. On the basis of these observations we conclude that libration of the C^α–C^β bond makes, at most, only a small contribution to the motion of the C^β–^2H bonds in A and B molecules and that the C^β–^2H bond reorientation is primarily due to rotation about the C^α–C^β bond axis.

Quantitative analysis of A and B molecule NMR data involves separating the overlapping powder patterns. Figure 5 shows composite and separated methionine line shapes at −1 and +60 °C. The separation procedure takes advantage of the different spin–lattice relaxation times (T_1) of the two patterns. The composite line shapes, Figure 5c, were acquired by using the quadrupole echo pulse sequence with recycle times, t, much greater than T_1 of both components. By choosing t so that $T_1^B \ll t \ll T_1^A$, the A molecule deuteron signals are selectively suppressed and the B molecule line shapes, Figure 5b, are obtained. Typically, ca. 85% of the A molecule signal could be suppressed in this manner. The A molecule line shapes, Figure 5a, are obtained by subtracting the (b) line shapes from the (c) line shapes. Although the T_1's of both the A and B molecules change with temperature, their difference is large at all temperatures studied and allows good signal separation.

The temperature dependence of the B molecule line shape is shown in Figure 6. The B line shape begins to depart from the static, $\eta = 0$, pattern at about −30 °C and coalesces to an $\bar{\eta} = 1$ pattern at +30 °C. At temperatures above 50 °C it is again nearly axially symmetric but is only one-half as wide as the static axially symmetric pattern observed at −35 °C.

The motions responsible for the changes in line shape have correlation times in the fast limit, $\tau \ll \omega_q^{-1} \sim 10^{-6}$ s. This conclusion is based upon the observation that varying the interval between 90° pulses in the quadrupole echo pulse sequence from 20 to 120 μs produced little intensity loss and no distortion of the powder line shape. In particular, the short, anisotropic T_2's characteristic of intermediate exchange, 10^{-4} s $\leq \tau \leq 10^{-6}$ s, were absent.[26] Inversion–recovery spectra obtained at 38.45 and 76.77

(25) Torii, K.; Iitaka, Y. *Acta. Crystallogr.* **1973**, *29*, 2799–2807.

(26) Spiess, H. W.; Sillescu, H. *J. Magn. Reson.* **1980**, *42*, 381–389.

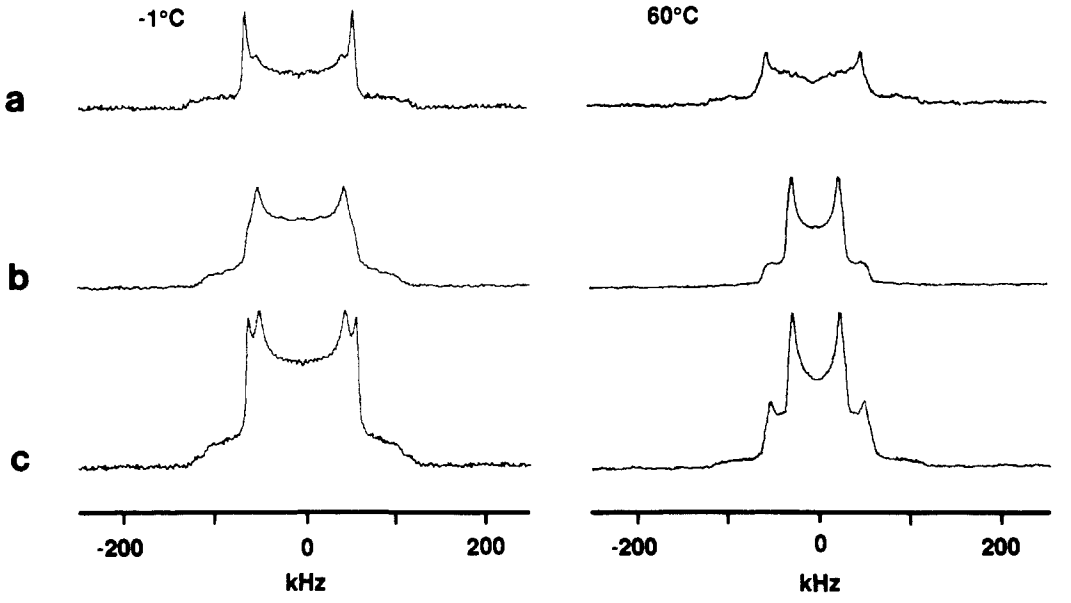

Figure 5. Separation of A and B molecule composite powder patterns in polycrystalline L-[3,3-$^2H_2$]methionine with T_1 discrimination. At −1 °C, the composite spectrum (c) and B molecule powder pattern (b) represent 1024 acquisitions each using 2 s and 75 ms recycle times, respectively. The corresponding spectra at 60 °C were acquired using 2 s and 335 ms recycle times. The A molecule line shapes (a) were obtained by subtraction of (b) from (c). Each measured spectrum was recorded at 38.45 MHz and symmetrized to facilitate the subtraction process. The ratio of A to B molecule relaxation times varied from approximately 70 at −1 °C to 9 at +77 °C. At the higher temperatures where line shape separation was more difficult, a choice of experiment recycle time $t = 3.5\ T_{1B}$ suppressed approximately 70% of the A molecule signal intensity, allowing B molecule principal frequencies to be measured. At higher temperatures, the principal frequencies of Table I were determined from composite line shapes.

MHz showed that T_1 was nearly field independent over most of the temperature range studied. Therefore, at 38.45 MHz, the correlation times of the B molecule C^β–^2H bonds are on the fast side of the T_1 minimum (i.e., $\tau \leq 10^{-9}$ s). Finally, the magic angle spinning ^{13}C spectra of L-methionine[27] show resolved peaks arising from A and B molecules. These spectra, which show a single narrow line for each A and B molecule carbon, are consistent with our conclusion that the A and B molecules execute side chain motions that are in the fast exchange limit.

In addition to providing information about the time scale of molecular motion, the NMR data allow us to estimate the minimum root-mean-square angular displacement of the C^β–^2H bond axis. For example, three distinctly different models of motion can all fit the high temperature, $\bar{\eta} = 0$, B line shape: (1) uniform diffusion in a cone, (2) uniform diffusion in a plane, and (3) two-site jumps. However, it is significant that one obtains essentially the same root-mean-square angle, $\theta_{rms} = 48 \pm 3°$, whichever model is used to fit the line shape.

Although we are able to obtain model independent estimates of motional correlation times and root-mean-square angles from the T_1 and line shape data, an appropriate motional model must be assumed in order to extract the additional information contained in this data. We have chosen the two-site jump model because of the following considerations. First, the X-ray data indicate that the low-energy conformations of the methionine side chain are either trans or gauche, and since we know that the methionine side chain, at least at high temperature, executes large-amplitude motion, we assign this motion to a trans-gauche or gauche-gauche isomerization. Since the barrier to such isomerization is typically 14 kJ/mol in liquids, the probability of finding a conformation in the vicinity of the potential maximum is small and a jump model is a reasonable approximation of the side chain motion.

We have assumed that the side chain jumps between only two sites because one set of B molecule averaged principal frequencies, those appearing at ±60 kHz, are almost completely insensitive to temperature, changing by less than 3 kHz over the 112 °C temperature range (Table I). This result is strong evidence that

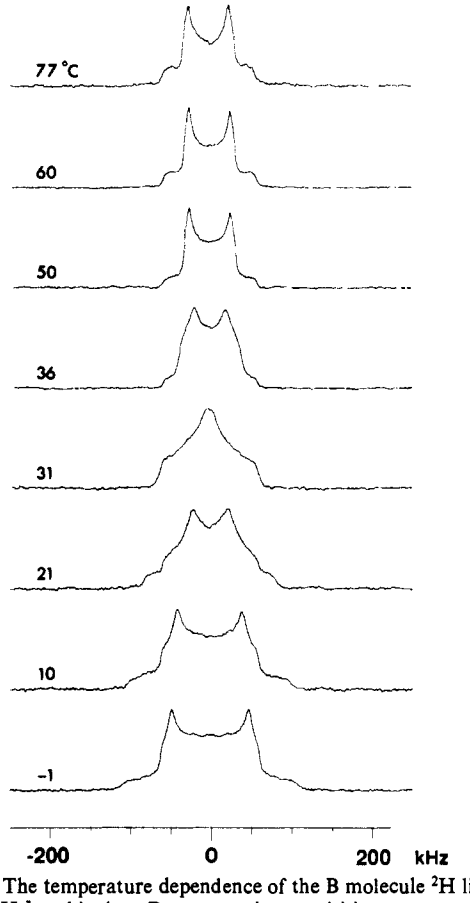

Figure 6. The temperature dependence of the B molecule ^2H line shape in L-[3,3-$^2H_2$]methionine. Representative acquisition parameters are the following: −1 °C, 1024 acquisitions, 75 ms recycle time ($T_{1A} \sim 0.7$ s, $T_{1B} \sim 11$ ms); +77 °C, 512 acquisitions, 435 ms recycle time ($T_{1A} \sim 0.8$ s, $T_{1B} \sim 87$ ms).

the C^β–^2H bond orientations are confined to a plane. In the case of fast limit planar motion, arguments similar to those in ref 28 show that the direction normal to the X_c,Z_c plane (Y_c in Figure 2) is a principal axis of the averaged EFG tensor. The corre-

(27) Diaz, L. E.; Morin, F.; Mayne, C. L.; Grant, D. M.; Chang, C. J. *Magn. Reson. Chem.* **1986**, *24*, 167–170.
(28) Jelinski, L. W.; Sullivan, C. E.; Batchelder, L. S.; Torchia, D. A. *Biophys. J.* **1980**, *10*, 515–529.

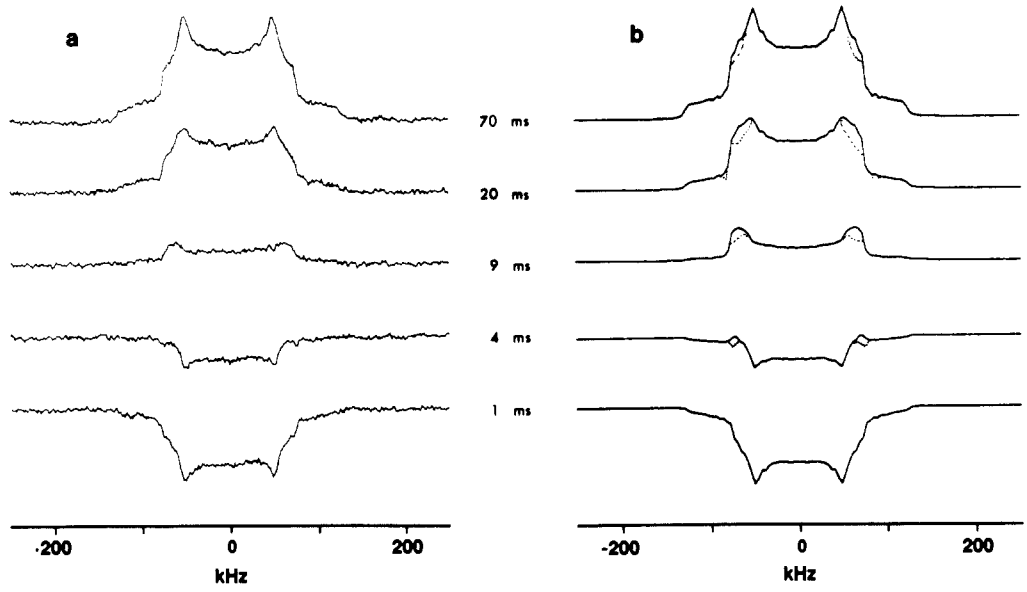

Figure 7. Experimental (a) and simulated (b) deuterium line shapes for B molecule deuterons in L-[3,3-$^2H_2$]methionine at 21 °C and 38.45 MHz. Small line shape intensity distortions, indicated in (b) with dotted lines, appear primarily between 50 and 60 kHz due to incomplete suppression of the A molecule deuteron signal.

Table II. L-[3,3-$^2H_2$]Methionine Squared Generalized Order Parameters[a] and Reorientational Correlation Times[b]

temp (°C)	temp^{-1} (10^3/deg K)	S_A^2	τ_A (ns)	S_B^2	τ_B (ns)
−19	3.937	0.992	0.450		
−15	3.876			0.920	4.14
−10	3.802			0.885	3.05
−1	3.676	0.983	0.175		
+1	3.650	0.985	0.225		
4	3.610			0.788	1.54
10	3.534			0.713	1.19
20	3.413	0.978	0.102		
21	3.401	0.980	0.080	0.514	0.705
31	3.289			0.333	0.450
36	3.236	0.915	0.050	0.258	0.230
50	3.096	0.873	0.032	0.251	0.120
60	3.003	0.842	0.028	0.251	0.080
62	2.985	0.866		0.251	
72	2.899	0.828		0.251	
77	2.857	0.799	0.019	0.251	0.049
82	2.817	0.799		0.251	
88	2.770	0.767		0.252	
106	2.639	0.686		0.253	

[a] Calculated using eq 5 and 6 and the principal frequencies in Table I. Estimates of error in S^2, 5–20%, were calculated using standard techniques. [b] Uncertainty in τ was calculated using eq 9 and the calculated uncertainty in S^2.

sponding principal frequency equals $\pm\nu_q/2$ (±60 kHz in the present case), independent of the amplitude of the motion, because B_0 is always orthogonal to the C–^{2}H bond when the field is along Y_c. Because reorientation of the C$^\beta$–^{2}H bond is due to rotation about the C$^\alpha$–C$^\beta$ bond, the tetrahedral geometry of carbon bonds requires that the rotational potential contain, at most, two low-energy minima, in order to confine the orientations of each C–^{2}H bond to one plane.

In order to determine S^2 for the two-site jump model, the motionally averaged principal frequencies, Table I, were measured in experimental spectra. The equilibrium line shapes were simulated by computer calculation by using the measured principal frequencies. Comparison of experimental with simulated line shapes revealed small intensity distortions in the B molecule line shapes at ca. ±60 kHz, due to incomplete saturation of the A molecule line shape (Figure 7). These distortions were found to have little influence on the values of S^2 obtained from eq 5 because the order parameter depends only upon the values of the principal frequencies and not the details of the line shape. With use of values of S^2, Table II, obtained from the equilibrium line

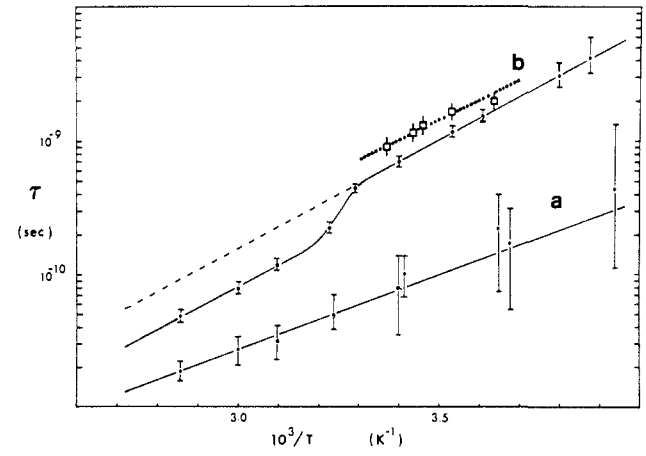

Figure 8. L-[3,3-$^2H_2$]Methionine methylene reorientation correlation times plotted as a function of inverse temperature. The A molecule correlation times (a), determined from 38.45-MHz data, indicate an apparent activation energy of 21.6 ± 8.3 kJ/mol. The B molecule correlation times (b), determined from 38.45-MHz data, show linearity in two regions. Below 31 °C, an apparent activation energy of 30.9 ± 1.6 kJ/mol is determined; above 50 °C, 30.9 ± 4.9 kJ/mol. The dashed line is present to facilitate comparison of correlation times and activation energies on either side of the methionine phase transition, 32–33 °C. The error estimates, two standard deviations, are discussed in the text. Open squares in trace (b) show correlation times determined from ratios of T_1's obtained at 76.77 and 38.45 MHz. An apparent activation energy of 29.0 ± 4.4 kJ/mol was calculated (dotted line).

shape principal frequencies, partly relaxed line shapes were calculated for a variety of inversion–recovery times, adjusting the correlation time until the calculated spectra matched those obtained experimentally. The correlation times obtained are listed in Table II and plotted against inverse temperature in Figure 8.

Random errors in correlation times were influenced by two factors. First, reasonable congruence of experimental and simulated spectra was obtained when correlation times were changed from the optimum value by 5–10% for a given set of principal frequencies. This contribution to the uncertainty in τ was similar for both A and B molecule line shapes and at all temperatures. A second source of error became important only when the deuterium line shape was nearly axially symmetric. This is clear from eq 8 and 9 where it is evident that, when $S^2 \simeq 1$, a small error in the measurement of S^2 produces a large error in the value of $(1 - S^2)$, and thereby in τ. The spectral signal-to-noise ratio, the deuterium signal line width, and the 500-Hz digital resolution limit

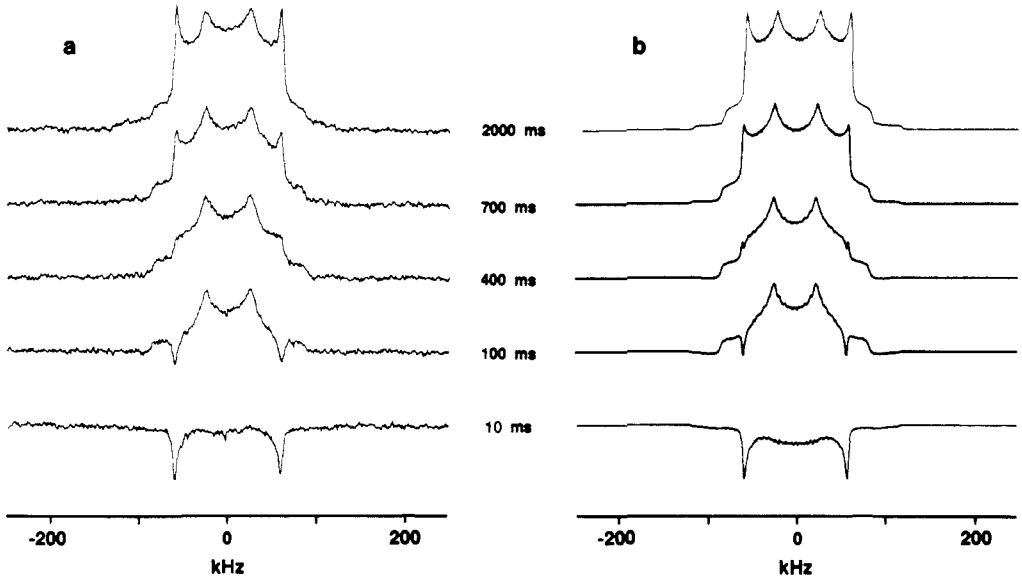

Figure 9. Experimental (a) and simulated (b) deuterium line shapes of L-[3,3-$^2H_2$]methionine. The experimental spectra are A and B molecule composite line shapes obtained at 21 °C and 38.45 MHz using a 2 s recycle time and the inversion–recovery delay times shown. The computer generated line shape simulations employ the order parameters and correlation times of Table II and Figure 8.

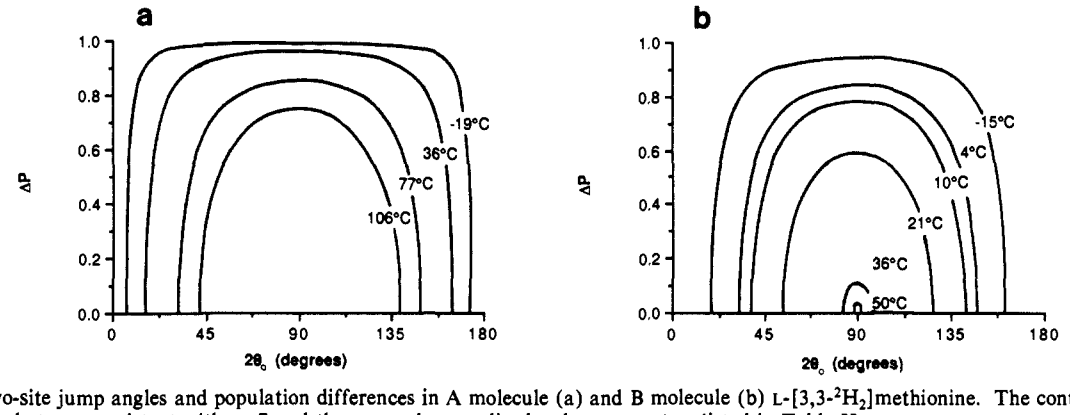

Figure 10. Two-site jump angles and population differences in A molecule (a) and B molecule (b) L-[3,3-$^2H_2$]methionine. The contours are values of ΔP and $2\Theta_0$ that are consistent with eq 7 and the squared generalized order parameters listed in Table II.

the accuracy with which the principal frequencies could be measured, contributing to the error estimates seen in Figure 8.

The trace of Figure 8b is linear in two temperature domains, permitting calculation of apparent activation energies from the 38.45-MHz data. Between −15 and +30 °C, the apparent activation energy for reorientation of the C^β–^2H bonds is 30.9 ± 1.6 kJ/mol. Above +50 °C, the apparent activation energy is 30.9 ± 4.9 kJ/mol. We note that the phase transition of L-methionine[12] occurs in the temperature range where the trace in Figure 8b is nonlinear.

We now turn our discussion to dynamics of the A side chains. The line shapes of the A molecules, like those of the B molecules, exhibit no T_2 distortion and have invariant principal frequencies at ±60 kHz. These observations indicate that the A molecule C^β–^2H bonds execute fast-limit two-site jumps like their B molecule neighbors. In spite of this similarity in their side chain dynamics, the A and B molecules exhibit significant differences in the values of their order parameters (Table II). The results summarized in Table II indicate that the root-mean-square amplitude of the C^α–C^β bond rotation is much smaller in the A molecule over virtually the entire temperature range.

Correlation times were determined for the A molecule C^β–^2H bonds, using values of S^2 listed in Table II, in the same manner as previously used for the B molecule. It should be noted again that when $S^2 \simeq 1$, it is difficult to determine τ accurately and that this condition is true for the A line shape throughout most of the temperature range studied. Consequently, large error estimates are associated with calculated values of τ_A. An additional source of error in τ_A is caused by the difficulty in observing an undistorted A molecule line shape between 10 and 40 °C. The extreme temperature sensitivity of the B molecule quadrupole splitting in this temperature range, seen in Figure 4, causes small temperature drifts during T_1 experiments to significantly distort the A molecule line shapes obtained from the subtraction procedure (Figure 5). The A molecule correlation times obtained in this temperature range were derived either from composite line shapes, using previously determined values for B molecule correlation times and principal frequencies, or from those T_1 experiments exhibiting favorable temperature stability. Figure 9 demonstrates the goodness of fit for composite inversion–recovery A molecule line shapes.

The apparent activation energy for the A molecules, obtained from Figure 8a, is 21.6 ± 8.3 kJ/mol. The large error limits associated with the correlation times may obscure nonlinear behavior in the case of the A molecule. It is clear that the apparent activation energy, the correlation times, and the order parameters that characterize the motion of the A side chains differ significantly from those of the B side chains. The differences in side chain dynamics are undoubtedly closely related to the difference in packing of the A and B side chains in the crystal lattice.

It is clear from eq 7 that measurement of S^2 provides information about the jump angle $2\Theta_0$ and the site populations, P_1 and P_2. Figure 10 shows that the measured order parameters are compatible with only a limited range of paired values of $2\Theta_0$ and ΔP, $\Delta P = |P_1 - P_2|$. Figure 10b shows that the order parameter of the B molecule observed at 50 °C is consistent only with equally populated jump sites, $\Delta P = 0.0 \pm 0.04$, and a jump angle of 90 ± 3°. Further, the B molecule order parameter, Table II, is nearly

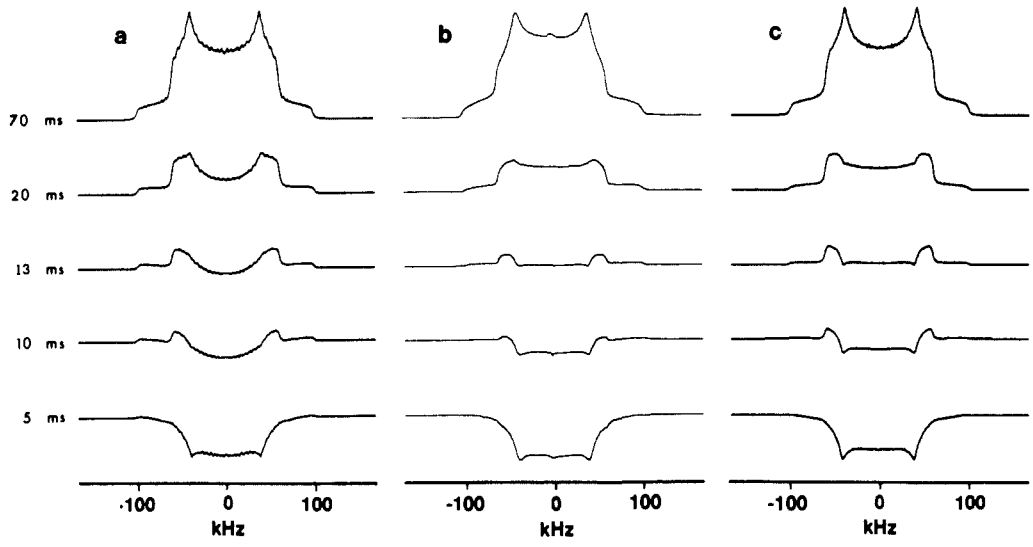

Figure 11. Comparison of experimental and calculated inversion–recovery ^2H NMR line shapes for L-[3,3-$^2H_2$]methionine. The experimental line shapes (b) were obtained at +10 °C and 76.77 MHz using a 70 ms recycle time and 4096 acquisitions. Computer simulated line shapes assume (a) two equally populated jump sites ($\Delta P = 0$, $2\theta_0 = 38.7°$) and (c) two unequally populated jump sites ($\Delta P = 0.78$, $2\theta_0 = 90°$). Other simulation parameters, S^2 and τ, are identical in (a) and (c). Note that parameter pairs in (a) and (c) correspond to different points on the 10 °C contour in Figure 10b.

constant between 50 and 106 °C, indicating that, within this temperature range, the site populations are nearly equal and the jump angle is ca. 90°.

At temperatures below 50 °C, the B molecule order parameters alone do not significantly restrict the range of possible values of ΔP and $2\Theta_0$. In order to determine these parameters, we measured spin–lattice relaxation times under conditions where the extreme narrowing condition, $(\omega\tau)^2 \ll 1$, was not satisfied, i.e., at 76.77 MHz and at temperatures below 24 °C.

Analysis of eq 8 shows that when $\omega\tau \geq 1$, the T_1 anisotropy predicted by the two-site jump model depends explicity upon ΔP and $2\Theta_0$, and not merely upon S^2. Figure 11, a and c, compares computer simulations of two-site jump inversion–recovery spectra calculated for two cases having equal values of S^2 and τ, but with $\Delta P = 0$, $2\Theta_0 = 39°$ and $\Delta P = 0.78$, $2\Theta_0 = 90°$, respectively. Although the average values of T_1 are the same in the two cases, the T_1 anisotropies are clearly different. In Figure 11b, the corresponding experimental spectra, measured at 10 °C, are clearly compatible only with the case of unequal site populations ($\Delta P = 0.78$, $2\Theta_0 = 90°$). Reasonable matching of experiment with simulation was obtained for $2\Theta_0 = 90 \pm 15°$ and $\Delta P = 0.76$–0.78. Additional 76.77-MHz inversion–recovery spectra, spanning the temperatures 2 to 24 °C, also show the T_1 anisotropy characteristic of 90° jump angles.

Although the two-site jump model correctly predicts the observed T_1 anisotropy using $2\Theta_0 = 90°$ and suitable values of ΔP and τ, the value of $\langle 1/T_1 \rangle$ ($\langle XX \rangle$ denotes the spherical average of XX) calculated using the same set of parameters is ca. 20% larger than the value of $\langle 1/T_1 \rangle$ measured in the 2–24 °C temperature range. In addition, if we use eq 8 together with the ratio of $\langle 1/T_1 \rangle$ values measured at 38.45 and 76.77 MHz to determine the correlation time at a particular temperature (in the 2–24 °C range) then the value of $\langle 1/T_1 \rangle$ calculated at either field strength using this correlation time (and the value of S^2 obtained from the principal frequencies) is ca. 20% larger than the observed $\langle 1/T_1 \rangle$.

The reason that the two-site jump model overestimates the value of $\langle 1/T_1 \rangle$ (when $\omega\tau \leq 1$) becomes clear when one compares the predictions of the jump model with the predictions of a more realistic model, diffusion in a potential.[29] First it is useful to compare the two models in the case of a potential with three minima having equal equilibrium populations (e.g., a methyl rotor) because the correlation function for the diffusion model has been worked out explicitly in this case.[29] From the point of view of NMR relaxation theory, the major difference between the diffusion and jump models is that the correlation function in the diffusion case is a summation of decaying exponentials (i.e., there is a distribution of correlation times) whereas in the jump model the correlation function decays as a single exponential. For potential barriers in excess of ca. 14 kJ/mol, the largest correlation time in the diffusion model, τ_1, corresponds approximately to the single correlation time, τ_3, in the three-site jump model. The other correlation times are much less than τ_1 and correspond to rapid, small amplitude, oscillations within the potential wells. These rapid motions do not produce significant spectral density at the Larmor frequency unless $(\omega\tau_1)^2 \gg 1$. It is for this reason that $\langle 1/T_1 \rangle$ calculated with use of the jump model is greater than $\langle 1/T_1 \rangle$ calculated with use of the diffusion model when $\omega\tau \leq 1$. For instance, for methyl group reorientation, $\langle 1/T_1 \rangle$ calculated with use of the jump model is 20% larger than $\langle 1/T_1 \rangle$ calculated with use of the diffusion model, provided that $\omega\tau \leq 1$, where τ equals either τ_1 or τ_3. Similar considerations apply to the two-site case and suggest that the two-site jump expression for $1/T_1$ be corrected by multiplying the right side of eq 8 by a correction factor which is slightly less than unity. Using an empirical value of 0.8 for the correction factor, we are able to fit all the relaxation data including the field dependence and anisotropy of T_1. The correlation times obtained with the modified form of eq 8 are listed in Table III and plotted as open squares in Figure 8. These correlation times are 20 to 40% larger than the correlation times obtained with the two-site jump model. Because the two sets of correlation times differ by about the same multiplicative factor at each temperature, they yield essentially the same apparent activation energies, 29 and 31 kJ/mol, respectively.

Although it is desirable to confirm the above arguments by using a double-well potential model[30] to calculate line shapes, such a calculation requires several days of VAX-750 computer time to obtain one set of partially relaxed spectra. We have therefore modeled the double-well potential using a six-site jump model. In this model the C–D bond orientations are defined by polar angles (Θ,Φ), where $\Theta = 70.5°$ for each site and $\Phi = \pm\Phi_0$, $\pm\Phi_0 + \Phi_1$, $\pm\Phi_0 - \Phi_1$. The two C–D bond orientations ($70.5° \pm \Phi_0$) correspond to the potential minima, and Φ_1 defines the extent of fluctuations (librations) within each potential. When $\Phi_0 = 48.6°$ and $\Phi_1 = 0°$, the six-site model reduces to the two-site model considered above, with $2\Theta_0 = 90°$. In all line shape calculations with the six-site model, the jump rate for the libration motion was assumed to be much greater (ca. 10^{11} s^{-1}) than the rate for jumps between the two minima, because the latter motion requires surmounting the potential barrier. Using the six-site model we were able to simulate the equilibrium and partially relaxed line shapes and T_1 field dependence observed at 10 °C using the

(29) Edholm, O.; Blomberg, C. *Chem. Phys.* **1979**, *42*, 449–464.

(30) Wittebort, R. J.; Olejniczak, E. T.; Griffin, R. G. *J. Chem. Phys.* **1987**, *86*, 5411–5420.

Table III. L-[3,3-$^2H_2$]Methionine B Molecule Correlation Times

temp (°C)	T_1 ratio[a]	τ_B[b] (ns)
+2	1.89	1.79
10	1.82	1.60 ± 0.10
16	1.72	1.38
18	1.60	1.21
24	1.39	0.90 ± 0.15
34	1.08	<0.50
45	1.00	

[a] $\langle 1/T_1\rangle$(76 MHz)/$\langle 1/T_1\rangle$(38 MHz). $\langle 1/T_1\rangle$ was determined from inversion-recovery spectra obtained at 76.77 or 38.45 MHz on B molecule deuterium line shapes. Experiment recycle times were chosen that allowed complete separation of A and B line shapes. No changes in partly relaxed B molecule spectra were observed when changing the recycle time by 30–50%. [b] Apparent activation energy E_a = 29.0 ± 4.4 kJ/mol (r = 0.98) was calculated using τ values of 10 to 24 °C.

following parameters: τ = 1.6 ± 0.2 ns (the correlation time for jumps between potential minima), Φ_{rms} = 8 ± 4° (the root-mean-square libration angle), ΔP = 0.80 ± 0.03 (the difference in populations of the two potential wells) and $2\Theta_0$ = 90 ± 15° (the angle made by the C–D bonds when their orientations correspond to the potential minima). The line shape simulation and the values of ΔP and $2\Theta_0$ derived by using the six-site model are virtually identical with results obtained with the two-site model. However, as a consequence of the inclusion of librational motion, τ derived from the six-site model is 33% larger than τ_B (Table II) and agrees with the correlation time derived from the T_1 field dependence (Table III). Therefore, in agreement with the qualitative argument presented earlier, the two-site model correctly characterizes the major features of the large-amplitude motion except that it yields an underestimate of τ.

The line shapes and relaxation times observed at 60 °C are also correctly calculated by using the six-site model with ΔP = 0 and $2\Theta_0$ = 90 ± 15°. However, Φ_{rms} could not be accurately determined at 60 °C because the calculated line shapes are not sensitive functions of Φ_{rms}. In addition, although the calculated T_1 is affected by a change in Φ_{rms} this change can be compensated for by adjusting τ. We have calculated an upper limit of Φ_{rms}, using a trigonometric double-well potential.[30] Calculated values of 7 and 13° were obtained for Φ_{rms} assuming respective potential barriers of 31 and 12 kJ/mol. Because the latter barrier height is less than one-half the measured value of 31 kJ/mol, 13° is considered to be the upper limit of Φ_{rms} at 60 °C. Using this value of Φ_{rms} in the six-site calculations yields τ = 0.10 ns, a correlation time that is 25% larger than listed in Table II. In summary, the values of τ_B, Table II, generally underestimate τ by a factor of ca. 0.8 because libration is neglected in the two-site model.

From our analysis of (a) the T_1 anisotropy observed at low temperature (≤24 °C) and (b) the line shapes observed at high temperature (≥50 °C), we find that the B molecule C$^\beta$–^{2}H bonds rapidly jump between two orientations that differ by ca. 90° throughout the entire temperature range studied. For tetrahedrally bonded carbon, bond directions differ by approximately 109°, so that the motion corresponds approximately to trans-gauche isomerization.

In contrast with the finding that the B molecule C$^\beta$–^{2}H bond jumps between sites whose relative orientations are independent of temperature, the difference in the relative populations of the two sites, ΔP, decreases abruptly as temperature increases from 0 to 40 °C. The plot of ΔP against temperature (Figure 12) shows that at temperatures above 40 °C a near equality of B molecule site populations is achieved. These results together with recent measurements,[13] which show that the methionine crystal unit cell volume increases by about 5% over the −20 to 94 °C temperature range, indicates that the populations (and therefore the free energies) of the two orientations of each C$^\beta$–^{2}H bond are nearly equal in the expanded crystal lattice at high temperature.

Examination of Figure 12 shows that at temperatures below 10 °C only one side chain conformation is significantly populated for each B molecule. The statement also applies to the A molecules. Evidently, the contracted crystal lattice at low temperatures causes the side chains of both the A and B molecules to adopt

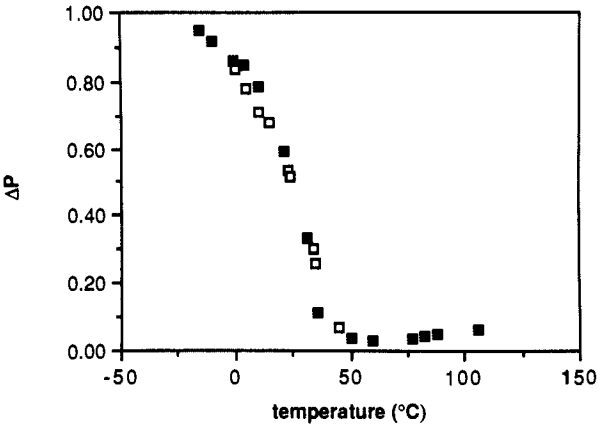

Figure 12. Jump site population difference, ΔP, versus temperature for B molecule L-[3,3-$^2H_2$]methionine. At temperatures below 0 °C, the trans (backbone N to C$^\gamma$) conformation is highly preferred.[25] Above 50 °C, the trans and one gauche conformer are nearly equally populated. The open squares represent values determined from 76.77-MHz data; the filled squares, 38.45 MHz.

the single conformations reported in the X-ray structure.[25]

The large decrease in the value of ΔP observed for the B molecules as temperature increases from 0 to 40 °C indicates that the rotational potential of the C$^\alpha$–C$^\beta$ bond changes in this temperature range. We therefore caution against interpreting the apparent activation energy measured below 50 °C as a barrier height. Above 50 °C, ΔP is nearly constant, indicating that the rotational potential for the B molecule side chain is temperature independent. Therefore the apparent activation energy measured above 50 °C, 30 kJ/mol, should be a good measure of the rotational barrier height. This value is about twice that typically measured for trans-gauche isomerization of alkane chains in liquids, probably as a consequence of the added steric hindrance exerted by neighboring atoms in the crystal lattice.

The ^{2}H line shape observed in the spectrum of L-[3,3-$^2H_2$]-methionine at −35 °C shows that large-amplitude motions of C$^\beta$–^{2}H bonds are absent at this temperature. However, the observed quadrupole splitting, 120 kHz, is smaller than the 128-kHz splitting typically observed at low temperature for methylene deuterons. This observation suggests that small-amplitude librational motions occur at −35 °C. We model this motion by assuming that the C$^\beta$–^{2}H bonds librate in a cone having a semiangle θ_c. Using eq 10 and a static quadrupole coupling constant of 128 kHz we obtain θ_c = 17° or equivalently θ_{rms} = 8°. We note that since θ_{rms} is small, the same value of θ_{rms} will be calculated for all models of motion in which the C$^\beta$–^{2}H bond moves in a potential having axial symmetry.[8,17]

A comparison of the order parameters of the A and B molecules, Table II, shows that the line shapes of the β-deuterons of the A molecules are not strongly averaged, even at temperatures above 80 °C. This result contrasts with the observation that the methyl ^{2}H line shapes of both the A and B molecules are strongly averaged at temperatures above 40 °C.[4] Evidently, motions involving rotations about the C$^\beta$–C$^\gamma$ and C$^\gamma$–S bonds cause a significant narrowing of the A molecule methyl line shape. In order to characterize the motion of the methionine side chain more fully, we are analyzing line shape and relaxation data of the amino acid deuteriated at the γ-carbon. Combining the results of the NMR and X-ray diffraction studies will provide detailed information about the interesting motions of the methionine side chain, which should serve as a model for possible motions of this side chain within proteins. In addition, the comprehensive NMR data obtained should provide a significant test for potential functions used in molecular mechanics calculations[2] of atomic trajectories.

Acknowledgment. We thank R. G. Tschudin for expert technical support and Dr. R. G. Griffin for the program used to calculate the six-site line shapes. This research was supported by NIH Grant RR08153.

Registry No. L-[3,3-$^2H_2$]Methionine, 113793-75-2.